New Type of Phase Transformation in Gas Hydrate Forming System at High Pressures. Some Experimental and Computational Investigations of Clathrate Hydrates Formed in the SF_6-H_2O System

E.Ya. Aladko,[†] A. I. Ancharov,[‡] S. V. Goryainov,[§] A. V. Kurnosov,[†] E. G. Larionov,[†] A.Yu. Likhacheva,[§] A.Yu. Manakov,*[,†] V. A. Potemkin,[||] M. A. Sheromov,[⊥] A. E. Teplykh,[#] V. I. Voronin,[#] and F. V. Zhurko[†]

Nikolaev Institute of Inorganic Chemistry, SD RAS, Ac. Lavrentiev ave. 3, Novosibirsk 630090, Russian Federation, Institute of Solid State Chemistry, SB RAS, Kutateladze str. 18, Novosibirsk 630128, Russian Federation, Institute of Geology and Mineralogy, SD RAS, Ac. Koptug ave. 3, 630090 Novosibirsk, Russian Federation, Chelyabinsk State University, Br. Kashirinyh str. 129, 454021 Chelyabinsk, Russian Federation, Budker Institute of Nuclear Physics, SB RAS, Ak. Lavrentieva ave. 11, Novosibirsk 630090, Russian Federation, and Institute of Metal Physics, UB RAS, S.Kovalevskoy st. 18, Yekaterenburg 620219, Russian Federation

Received: March 19, 2006; In Final Form: August 11, 2006

In this work, we present a new, previously unknown type of structure transformation in the high-pressure gas hydrates, which is related to the existence of two different isostructural phases of the sulfur hexafluoride clathrate hydrates. Each of these phases has its own stability field on the phase diagram. The difference between these hydrates consists of partial filling of small D cages by SF_6 molecules in the high-pressure phase; at 900 MPa, about half of small cages are occupied. Our calculations indicate that the increase of population of small cavities is improbable, therefore, at any pressure value, a part of the cavities remains vacant and the packing density is relatively low. This fact allowed us to suppose the existence of the upper pressure limit of hydrate formation in this system; the experimental results obtained confirm this assumption.

Introduction

Clathrate hydrates present the inclusion compounds in which host framework is composed of hydrogen-bonded water molecules, and polyhedral cavities of this framework can include a wide range of guest molecules from hydrogen and helium to large organic molecules. In the case of gaseous (under normal conditions) guest molecules, these compounds are usually called gas hydrates. At moderate pressures (tens of MPa), a majority of them belongs to three structure types: two cubic (cubic structure I or CS-I, cubic structure II or CS-II)[1,2] and one hexagonal structure H.[3,4] The hydrate frameworks of all these structures contain several types of polyhedral cavities: D (5^{12}, a polyhedron with 12 pentagonal faces) and T ($5^{12}6^2$) for CS-I, D and H ($5^{12}6^4$) for CS-II, and D, D′ ($4^35^66^3$), and E ($5^{12}6^8$) for structure H. The structures of these hydrate frameworks were discussed in the literature for many times, therefore, we do not consider this in detail here. We should only mention that the difference in dimensions of the framework cavities is minimal for CS-I.

At elevated pressure, new hydrates with denser lattice packing are formed in many systems. Recently, numerous structural and physicochemical studies were performed on the hydrates formed in the systems water−nitrogen,[5−7] hydrogen,[8−10] rare gases,[11−15] methane,[16−19] and some others. For example, the existence of four hydrates with different structure was established in the system argon−water up to 3 GPa.[13,20] The argon hydrate CS-II existing at the atmosphere pressure is stable up to 460 MPa. At 460−760 MPa, the H-type hydrate exists, with the large cavities filled by five ordered atoms of argon. The hydrates existing above 760 MPa belong to fundamentally new structure types. In these structures, all the argon atoms have the same water environment, i.e., both structures may be presented as an association of polyhedral cavities of one type.[13,20] The hydrates of this type are also found in the systems methane−water[19] and tetrahydrofuran−water.[21] Even such a brief survey of literature shows the insufficiency of structural studies of high-pressure hydrates in the systems with relatively large guest molecules. The available data are actually restricted to the two works,[21,22] which defines our interest to these studies.

The system hexafluoride−water presents a large class of systems with characteristic size of a guest molecule of about 6 Å, in which the clathrate hydrates CS−II are formed at atmospheric pressure. The guest molecules occupy only the large framework cavities (1 molecule per cavity) and the small cavities are vacant. Typical stoichiometry of these hydrates is $G*17H_2O$. Figure 1 shows a P−T projection of the phase diagram of the system hexafluoride−water.[23] The bends of the melting curve indicate that at least three hydrates are formed in this system up to 1.3 GPa. The hydrate h_1 (CS-II with composition $SF_6 \cdot 17H_2O$[24,25]) is stable up to 33.2 MPa; at higher pressure, the decomposition branch $l_1h_1l_2$ of this hydrate is traced up to 58 MPa (10.5 °C), i.e., to the metastable P,T region. Upon melting−recrystallization cycling or long exposure at these P,T conditions, another phase h_2 crystallizes. As we demonstrated earlier,[26] this

* Corresponding author. E-mail: manakov@che.nsk.su. Telephone: (7-383) 339 13 46. Fax: (7-383) 330 94 89.
[†] Nikolaev Institute of Inorganic Chemistry.
[‡] Institute of Solid State Chemistry.
[§] Institute of Geology and Mineralogy.
[||] Chelyabinsk State University.
[⊥] Budker Institute of Nuclear Physics.
[#] Institute of Metal Physics.

10.1021/jp061698r CCC: $33.50
Published on Web 09/21/2006

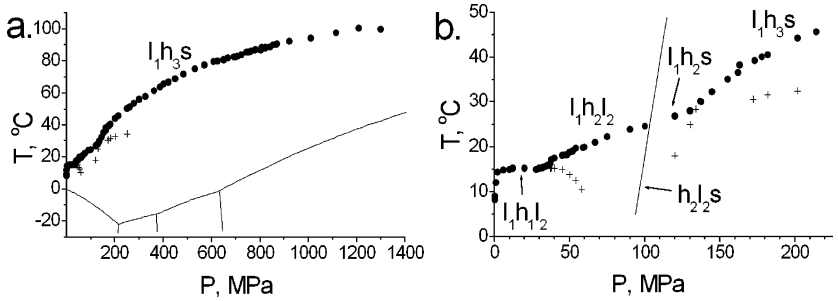

Figure 1. Phase diagram of SF_6-H_2O system.

hydrate has the structure CS-I. The decomposition curve $l_1h_2l_2$ of this hydrate lies within 33.2−131.9 MPa. From the data of ref 27, it follows that, at 92.0 MPa and 24.3° C, this curve must intersect the melting curve l_2s of solid sulfur hexafluoride, which implies the appearance of quadrupole point $l_1h_1l_2$s in the system. The decomposition curve of hydrate h_2 bends sharply at 131.9 MPa, which denotes the appearance of new hydrate h_3. The incongruent decomposition of hydrate h_2 (metastable branch l_1h_1s) was observed up to 201.5 MPa, i.e., far above the stability field of this hydrate. The decomposition curve of hydrate h_3 is investigated up to 1.3 GPa. Earlier, we performed the diffraction studies of the SF_6 hydrates in the stability field of this hydrate.[26] All the obtained diffractograms corresponded to CS-I type, i.e., the structure of hydrate h_2. The most plausible explanation for this observation was a metastable existence of the hydrate h_2 in the stability field of the hydrate h_3. However, a significant overpressurization (up to 450 MPa above the estimated pressure of transition) was surprising, taking into account that the curve of metastable decomposition for hydrate h_2 was traced only to 201.5 MPa. The aim of the present work is to clarify the hydrate formation in this pressure region.

Experiment

The neutron diffraction experiments were performed using a piston−cylinder apparatus for in situ measurements.[28] Neutron powder diffraction patterns were collected at room temperature and 80 and 900 MPa at research reactor IVV-2M (Yekaterinburg)[29] using a monochromatic neutron beam with $\lambda = 1.5246$ Å. Finely powdered ice was loaded in the apparatus chamber at liquid nitrogen temperature, and then sulfur hexafluoride was condensed. An excess of solid hexafluoride was used as a pressure-transmitting medium.

Synchrotron X-ray diffraction experiments were carried out on the fourth beamline ($\lambda = 0.3675$ Å) at the VEPP-3 synchrotron source of the Budker Institute of Nuclear Physics SD RAS (Novosibirsk).[30] Synchrotron X-ray diffraction patterns were collected at room temperature and 50−600 MPa using a piston−cylinder apparatus with a beryllium window for in situ measurements.[31] Hydrate was synthesized directly in the working volume of the apparatus from powdered ice and sulfur hexafluoride at P,T of 1 MPa and −10 °C, respectively. In both cases, the pressure was controlled by measuring the force applied to the piston.

Raman spectra were recorded with a DILOR OMARS 89 spectrometer equipped with a CCD Princeton Instruments LN/CCD1100PB detector. The 514.5 nm line of an argon ion laser was used for excitation. The detector was calibrated with the characteristic lines of a neon lamp. The uncertainty in the position of spectral bands was $\Delta\nu = \pm 0.5$ cm^{-1}. A detailed description of the high-pressure diamond anvil cell is given in ref 32. Pressure in the cell was measured from the pressure shift of the R_1 and R_2 lines of ruby fluorescence using the pressure scale proposed in ref 33 ($\Delta\nu = \pm 0.5$ cm^{-1} corresponds to the error in the pressure determination of ±0.07 GPa). DAC was loaded with a powder of SF_6 hydrate, which was prepared at P,T of 0.5 MPa and −5 °C, respectively, in the low-pressure apparatus.

Calculations

The computational modeling was performed within the force field MERA.[34,35] This approach presents the potential energy of interactions as a sum of intra- and intermolecular coulomb and van der Waals interactions. The intra- and intermolecular Coulomb energies were calculated by a common formula. The energy of van der Waals interactions was calculated using the Lennard-Jones potential:

$$E_V = \sum_{i=1}^{N} \sum_{j=i+1}^{N} \left(-2U_{ij}\left(\frac{R_{ij}^e}{R_{ij}}\right)^6 + U_{ij}\left(\frac{R_{ij}^e}{R_{ij}}\right)^{12} \right)$$

where R_{ij}^e = equilibrium distance of van der Waals contact of atoms i and j equal to the sum of their van der Waals radii calculated in MERA.[34] Here the value U_{ij} corresponds to the minimum depth of potential energy of the interaction between atoms i and j and is calculated within the MERA model by formula:[35]

$$U_{ij} = \frac{7kR_{ij}^e}{48\alpha}$$

where α = constant equal to $6.662 \cdot 10^{-14}$ m/K; k = Boltzman constant. The energy of intermolecular hydrogen bonds was calculated according to

$$E_{VI} = \sum_{k=1}^{\infty}\sum_{l=1}^{\infty}\sum_{m=1}^{\infty}\sum_{i=1}^{M}\sum_{j=1}^{M} p_{ij}\left(-2U_{ij}R_{ij}^{e6}\left(\frac{1}{(R_{ij}+ka)^6} + \frac{1}{(R_{ij}+lb)^6} + \frac{1}{(R_{ij}+mc)^6}\right) + U_{ij}R_{ij}^{e12}\left(\frac{1}{(R_{ij}+ka)^{12}} + \frac{1}{(R_{ij}+lb)^{12}} + \frac{1}{(R_{ij}+mc)^{12}}\right)\right)$$

where a, b, c = cell parameters, $k = 0, 1, 2, 3...$. To correlate the system energy and the filling of small cavities by SF_6 molecules, the population of small cavities within one unit cell (nine small cavities) was varied. All the large cages were assumed to be fully occupied. We considered different combinations of the occupied sites within one unit cell with additional variation of orientation of SF_6 molecules in small cages and further optimization of orientational characteristics for all the molecules in the unit cell (SF_6 and H_2O). The genetic algorithm[35]

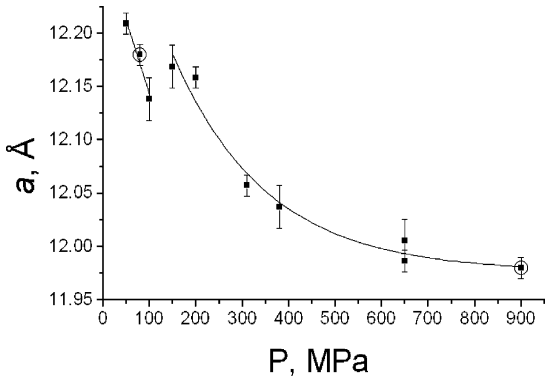

Figure 2. Pressure dependence of lattice constant of hydrates h_1 and h_2 based on X-ray and neutron diffraction measurements. Neutron data are marked by rings.

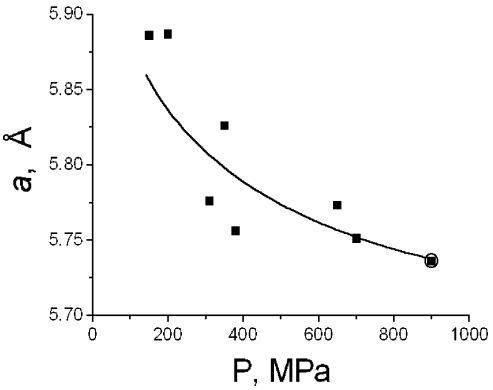

Figure 3. Pressure dependence of lattice constant of pure SF_6. Neutron data are marked by ring.

was used to vary the population and the orientation. The optimization of orientational characteristics for all the molecules in the cell was performed using quasi-Newtonian methods. The calculations were performed for one unit cell as approximation to quasi-infinite crystal, i.e., all the crystal cells were assumed to be equivalent.

Results and Discussion

A. Preliminary Studies. The pressure dependence of the unit cell parameters for hydrates h_2 and h_3 (Figure 2) was obtained from a series of the X-ray powder diffraction patterns of hydrates in the system hexafluoride−water collected at 50−650 MPa. It should be noted that, in the course of these experiments, we have corrected a methodic mistake that led to a systematic shift of the unit cell parameters in our previous work.[26] The data presented in this work are correct and fairly agree with the corresponding data of neutron diffraction experiments (see below). The unit cell of hydrate turned out to correspond to the gas hydrate structure CS-I up to 650 MPa. However, at about 130 MPa, the compressibility curve exhibits a discontinuity, which indicates the phase transformation in the system. Thus, all the obtained data indicated the existence of two hydrate phases related to one structure type. Such an unusual situation will be discussed later. In this section, we should mention one more result of these preliminary studies. Because the samples for diffraction experiments were prepared with an excess of sulfur hexafluoride, the diffraction patterns obtained under the conditions of stability of solid SF_6 contained the reflections of this compound. The reflections positions corresponded to those expected for the volume-centered cubic cell of plastic phase SF_6.[36] The reflection (110) did not overlap with the other reflections in the pattern, which allowed us to estimate the unit cell parameters for this phase at several pressure values (Figure 3). In the case of neutron diffraction pattern (point at 900 MPa), the unit cell parameter was determined by means of Rietveld refinement.

B. Neutron Diffraction Data. To elucidate the difference between the two considered hydrate phases, we have studied the neutron powder diffraction patterns of hydrate h_2 at 80 MPa and hydrate h_3 at 900 MPa (Figure 4). In both patterns, the reflections positions correspond to hydrate CS-I, with additional reflections of solid sulfur hexafluoride in the h_3 pattern. In these experiments, we used a high-pressure chamber of large volume (working volume about 1.5 cm^3) and finely ground ice as a reagent for hydrate preparation. This allowed us to obtain the neutron diffraction patterns of good quality suitable for Rietveld refinements of the hydrates structures. Starting coordinates for the framework water atoms were taken from ref 37, and their displacement parameters were as those of ice in similar conditions.[38,39] The preferred orientation correction was not made. The displacement parameters for sulfur and fluorine atoms were as for the framework atoms. This is because, from volumetric considerations, the molecules of sulfur hexafluoride are assumed to fill the framework cavities as tightly as possible. Selected results of Rietveld refinements are listed in Table 1.

The refined coordinates and displacements parameters of the framework atoms do not differ significantly with those from the literature data. The pressure-induced changes in the host framework are related mainly to the hydrogen bond distance; no distortion of the angles between hydrogen bonds is observed (Table 1). There are no signs of superstructure formation. We examined different possible orientations and populations of guest molecules in cavities. Regarding the large T cages, a partially ordered arrangement of the SF_6 molecules (Figure 5) proved to be a most adequate model. The SF_6 molecule was taken as a rigid model in this case. The position of sulfur atom is close to the cavity center. Refinement of different positions of fluorine atoms has shown that nonzero occupations occurs for two atoms that are situated at the line connecting centers of hexagonal faces of the T cavity (axial atoms) and four atoms in the equatorial plane. Axial fluorine atoms are directed to the centers of hexagonal faces, their positions being probably fixed by hollows in these faces. Four equatorial fluorine atoms are disordered in the equatorial plane. Occupation of other types of possible positions of fluorine atoms was found to be almost zero, and in the final refinement cycles, corresponding occupations were fixed as zero.

The SF_6 molecule in small cages was modeled by the sulfur atom in the cavity center and disordered fluorine atoms around it at the distance corresponding to the covalent S−F bond. The best fit for the hydrate h_2 was achieved in the case of empty small cages. For hydrate h_3, the population of small cages was set and fixed at the beginning of the refinement cycle, with subsequent refinement of all the atomic coordinates. Figure 6 shows the correlation between *R* factor and population of small cages. The best coincidence between the model and the experimental data was achieved at partial (about 50%) filling of small D cages by SF_6 molecules.

To ensure the completion of transition to stable phase h_3 at 130 MPa, we have lowered the pressure down to 100 MPa and then raised the temperature in the high-pressure chamber to 60 °C with further increase of pressure up to 900 MPa and cooling to room temperature. In this way, we stimulated the crystallization of hydrate h_3 from solid SF_6 and liquid D_2O, which excludes a metastable formation of hydrate h_2. The neutron

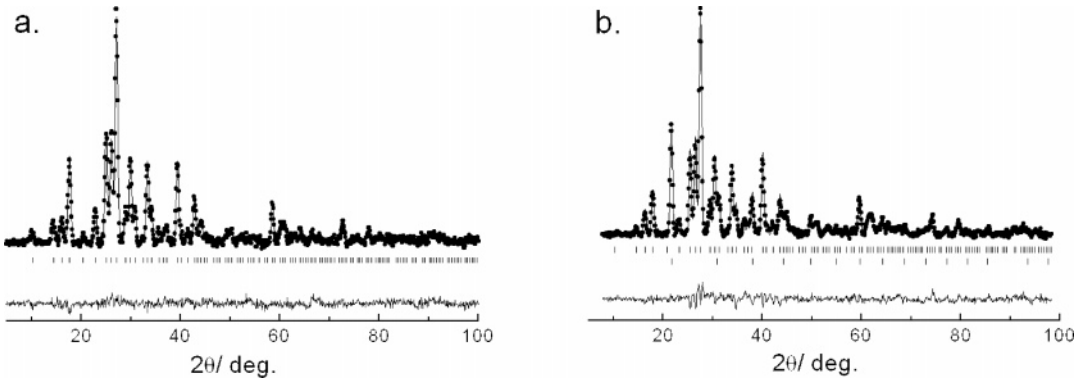

Figure 4. Powder diffraction patterns of hydrate h_2 at 80 MPa and room temperature (a) and h_3 at 900 MPa and room temperature (b). Experimental data and calculated pattern are shown by rings and solid line, respectively. Calculated positions of reflections are shown by sticks. The difference between the observed and calculated intensities is shown by the bottom solid line. In pattern (b), the reflections from solid sulfur hexafluoride are shown in the bottom row.

TABLE 1: Some Refined Parameters of SF_6 Clathrate Hydrates h_2 and h_3

	h_2	h_3
pressure, MPa	80	900
space group	*Pm*3*n*	*Pm*3*n*
unit cell parameter, Å	12.18(1)	11.98(1)
hydrate stoichiometry	$SF_6 \cdot 7.67H_2O$	$SF_6 \cdot 6.57H_2O$
calculated density, g/cm^3	1.567	1.785
y[a]	0	0.5
R, %	10.9	10.0
interatomic distances		
O−O, Å	2.77−2.90	2.69−2.81
O−F, Å (large cavities)	>3.2	>3
O−F, Å (small cavities)		2.62−3.15
angles		
O−O−O, deg	106−123	105−125

[a] y: Degree of occupation of small D cavities by SF_6 molecules.

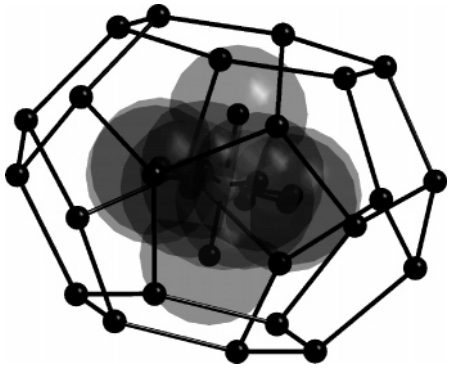

Figure 5. SF_6 molecule in large cavity of CS−I structure.

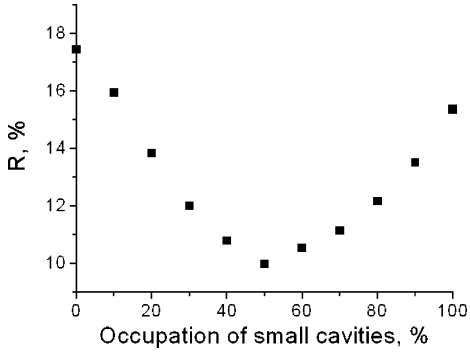

Figure 6. Dependence of R factor vs filling of small cavities.

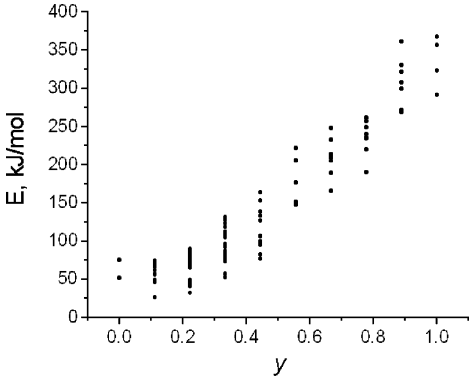

Figure 7. Calculated internal energy of SF_6 hydrate vs filling of small cavities.

diffraction pattern of the hydrate h_3 obtained through this procedure appeared to be the same as that of hydrate h_3 obtained previously.

Thus, the neutron diffraction data show that the phase transition observed in the system SF_6-H_2O at 130 MPa and 28.2 °C (quadrupole point, Figure 1) is associated with pressure-induced abrupt filling of a part of small cages of hydrate h_2 by the SF_6 molecules. Both hydrate phases belong to the same structure type CS-I. It should be mentioned that the entering of such a large molecule as SF_6 (6 Å in diameter) in a small D cage (free diameter 5.2 Å[40]) seems surprising. To "legitimize" these experimental results, we have performed a series of calculations.

C. Calculations. Figure 7 presents the calculated energies of the unit cell (the sums of intra- and intermolecular interactions for 1 mol of cells) for hydrate h_3 at 150 MPa at different values of the small cages occupation by sulfur hexafluoride (y). Because of a rather "dense" arrangement of guest molecules in the cavity, the potential energy surface here has many local minima with appreciable difference in energies. To a good accuracy, one can consider the orientations of the SF_6 molecules in small cages to correspond to those having minimal energy. It is seen that, at $y < 0.33$, the entry of the SF_6 molecules does not lead to the increase of internal energy of the hydrate, whereas at $y > 0.5$, the energy value grows rapidly. Probably, at relatively low y values, the volume increase of the occupied D cages is compensated by the framework deformation and compression of vacant cages, which becomes impossible at higher y values. Thus, at $y < 0.5$, the filling of small D cages by SF_6 molecules does not lead to a significant growth of the internal energy of the hydrate, which apparently makes possible the considered phase transformation. Besides, one could mention two more factors which favor the filling of D cages by guest molecules. First, this is an increase of configurational entropy of the hydrate

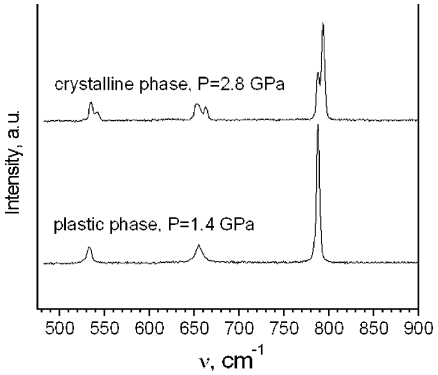

Figure 8. Typical Raman spectra of plastic and crystalline SF_6.

with partially filled cavities. The second factor is the free energy gain in term *PV* at the expense of the volume reduction at the absorption of the guest by the hydrate. According to our data (Figure 3), at 150 MPa, the molar volume of pure sulfur hexafluoride is 60.9 cm^3, which gives $PV = 9.1$ kJ/mol, increasing up to 51.3 kJ/mol at 900 MPa. It is interesting that the considered phenomenon has much in common with the overhydration effect observed in some zeolites.[41] For example, upon compression of natrolite in a water medium, additional water molecules enter the zeolite cavities, which results in the volume expansion of the solid phase and the reduction of the overall system volume. A more detailed theoretical modeling of the considered phase transformation is beyond the frame of this work and is a subject of future study.

As indicated above, at $y > 0.5$, free energy of the system rises rapidly with the increase of population of small cages; the achievement of higher population seems improbable at any pressure value. To date, only two examples of clathrate hydrates existing above 5 MPa are described in the literature: these are hydrates of hydrogen[8] and methane.[19] The structures of these compounds do not resemble classic structures of clathrate hydrates. A good "match" between the dimension and form of the cavities and those of the guest molecules seems to be an important factor that allows these hydrates to exist in a large pressure range. Such an adjustment provides a gain in the lattice packing as compared to the individual components phases. If this adjustment requires too strong distortion of the framework, an effective lattice packing becomes impossible. Therefore, at a certain pressure value, the upper pressure limit of hydrate existence is achieved, as it was observed in several cases.[20,42] As discussed above, the structure of hydrate h_3 will always contain some part of vacant cavities, which allows us to expect the existence of the upper pressure limit of hydrate formation for this system as well. We have checked this assumption by means of Raman spectroscopy in the high-pressure diamond anvil cell.

D. Raman Spectroscopy. The comparison of limited literature data on the phase diagram of pure sulfur hexafluoride[27,36,43,44] allows us to conclude that, at room temperature, liquid-phase SF_6 exists below 90 MPa, a plastic volume-centered phase SF_6 exists in the pressure range of 90 MPa to 1.6 GPa, transforming to crystalline phase at higher pressures. Our Raman spectra of pure sulfur hexafluoride are in satisfactory agreement with these literature data (Figures 8, 9). The Raman spectrum of sulfur hexafluoride contains three active modes: ν_1 at 775 cm^{-1}, ν_2 at 643 cm^{-1}, and ν_5 at 524 cm^{-1}. The pressure dependence was obtained for the strongest mode ν_1 (Figure 9). The phase transition in solid hexafluoride is marked by the splitting of all three bands at about 1.9 GPa (Figure 8) and

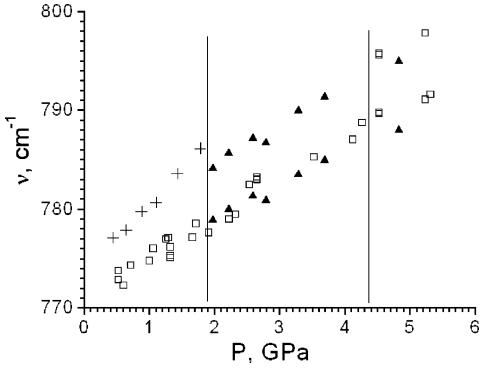

Figure 9. Pressure dependence of wavenumber of the ν_1 band in the Raman spectra of SF_6 in (+) plastic phase, (□) clathrate phase, (▲) crystalline phase. Vertical lines correspond to the pressures at which plastic−crystalline phase transformation (left) and decomposition of clathrate hydrate take place.

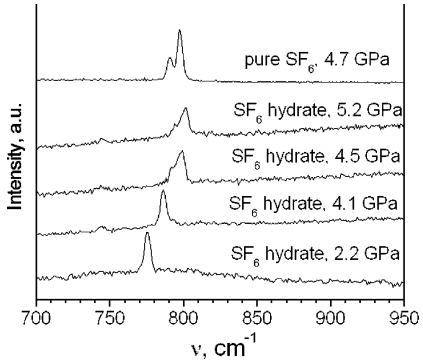

Figure 10. Typical Raman spectra of SF_6 clathrate hydrate and pure SF_6 at different pressures.

change of the slope of their pressure dependence curves (shown at Figure 9 for the band ν_1).

Because of a relatively low concentration of sulfur hexafluoride in the hydrate and weakness of the corresponding Raman bands, we have obtained the pressure dependence only for the strongest band ν_1, which probably corresponds to the vibrations of SF_6 molecules in large cavities. Typical spectra are presented in Figure 10. The absence of band splitting in the spectrum of hydrate phase due to the presence of two kinds of cavities may be explained by the intimate environment of the SF_6 molecule in a small cage and, as a consequence, a strong smearing of the S−F vibrations bands. Besides, the SF_6 concentration in small cages is at least 6 times lower as compared to large cages. The linear shift of the band ν_1 in the hydrate spectrum at 0.6−4.4 GPa (Figure 9) evidences the absence of phase transitions at these conditions, i.e., the absence of new hydrate phases. At about 4.4 GPa, the band splitting occurs; at higher pressures, the observed spectrum is in satisfactory agreement with that of solid sulfur hexafluoride (Figure 10). This may be related only with the decomposition of the hydrate to solid sulfur hexafluoride and ice VII, stable at these conditions. Thus, at room temperature, the upper pressure limit of hydrate formation in the system sulfur hexafluoride−water lies at about 4.4 GPa.

Conclusions

The experimental results of this work indicate the existence of a previously unknown type of phase transformation in the high-pressure clathrate hydrates. It has been found that two different phases of clathrate hydrates of sulfur hexafluoride, having their own stability fields on the phase diagram, belong to the same structure type CS-I. The difference between these

hydrates consists of partial filling of small D cages of the hydrate framework by SF_6 molecules in the high-pressure phase; for example, at 900 MPa, about half of the small cages are occupied. Our calculations show that the achievement of higher degrees of population is energetically unfavorable, i.e., at any pressure value, a part of the hydrate framework cavities remains vacant and the lattice packing is relatively loose. This fact allows us to suppose the existence of the upper pressure limit of hydrate formation in this system; the presented experimental results are evidence for the existence of this pressure limit.

Acknowledgment. This work is supported by the Intergration project of SD RAS 03-43.

References and Notes

(1) Sloan, E. D., Jr. *Clathrate Hydrates of Natural Gases*, 2nd ed.; Marcel Dekker: New York, 1997.

(2) Jeffrey, G. A. Hydrate Inclusion Compounds. In *Comprehensive Supramolecular Chemistry, Vol. 6, Solid-State Supramolecular Chemistry: Crystal Engineering*; Atwood, J. L., Davies, J. E. D., MacNicol, D. D., Vogtle, F., Eds.; Elsevier Science Ltd.: Oxford: 1996, p 757.

(3) Ripmeester, J. A.; Tse, J. S.; Ratcliffe, C. I.; Powell B. M. *Nature* **1987**, *325*, 135.

(4) Udachin, K. A.; Ratcliffe, C. I.; Enright, G. D.; Ripmeester, J. A. *Supramol. Chem*. **1997**, *8*, 173.

(5) Chazallon, B.; Kuhs, W. F. *J. Chem. Phys*. **2002**, *117*, 308.

(6) Dyadin, Yu. A.; Larionov, E. G.; Aladko, E. Ya.; Zhurko, F. V. *Dokl. Phys. Chem*. **2001**, *378* (4−6), 159.

(7) Hinsberg, M. G. E.; Scheerboom, M. I. M.; Schouten, J. A. *J. Chem. Phys*. **1993**, *99*, 752.

(8) Vos, W. L.; Finger, L. W.; Hemley, R. J.; Mao, H. *Phys. Rev. Lett*. **1993**, *71* (19), 3150.

(9) Dyadin, Yu. A.; Larionov, E. G.; Manakov, A. Yu.; Zhurko, F. V.; Aladko, E. Ya.; Mikina, T. V.; Komarov, V. Yu. *Mendeleev Commun*. **1999**, 209.

(10) Lokshin, K. A.; Zhao, Y.; He, D.; Mao, W. L.; Mao, Ho−Kwang; Hemley, R. J.; Lobanov, M. V.; Greenblatt, M. *Phys. Rev. Lett*. **2004**, *93*, 125503-1.

(11) Dyadin, Yu. A.; Larionov, E. G.; Aladko, E. Ya.; Manakov, A. Yu.; Zhurko, F. V.; Mikina, T. V.; Komarov, V. Yu.; Grachev, E. V. *Russ. J. Struct. Chem*. **1999**, *40*, 790.

(12) Loveday, J. S.; Nelmes, R. J.; Klug, D. D.; Tse, J. S.; Desgreniers, S. *Can. J. Phys*. **2003**, *81*, 539.

(13) Manakov, A. Yu.; Voronin, V. I.; Kurnosov, A. V.; Teplych, A. E.; Komarov, V. Yu.; Dyadin, Yu. A. *J. Inclusion Phenom*. **2004**, *48*, 11.

(14) Sanloup, C.; Mao, H.-K.; Hemley, R. J. *Proc. Natl. Acad. Sci. U.S.A.* **2002**, *99*, 25.

(15) Lots, H. T.; Schouten, J. A. L. *J. Chem. Phys*. **1999**, *111*, 10242.

(16) Dyadin, Yu. A.; Aladko, E. Ya.; Larionov, E. G. *Mendeleev Commun*. **1997**, 34.

(17) Loveday, J. S.; Nelmes, R. J.; Guthrie, M. *Nature* **2001**, *410*, 661

(18) Hirai, H.; Tanaka, T.; Kawamura, T.; Yamamoto, Y.; Yagi, T. *Phys. Rev. B* **2003**, *68*, 172102-1.

(19) Loveday, J. S.; Nelmes, R. J.; Guthrie, M.; Klug, D. D.; Tse, J. S. *Phys. Rev. Lett*. **2001**, *87*, 215501-1.

(20) Hirai, H.; Tanaka, T.; Kawamura, T.; Yamamoto, Y.; Yagi, T. *J. Chem. Phys*. **2002**, *106*, 11089.

(21) Kurnosov, A. V.; Komarov, V. Yu.; Voronin, V. I.; Teplych, A. E.; Manakov, A. Yu. *Angew. Chem., Int. Ed*. **2004**, *116*, 2982.

(22) Zakrzewski, M.; Klug, D. D.; Ripmeester, J. A. *J. Incl. Phenom*. **1994**, *17*, 237.

(23) Dyadin, Yu. A.; Larionov, E. G.; Manakov, A. Yu.; Kurnosov, A. V.; Zhurko, F. V.; Aladko, E. Ya.; Ancharov, A. I.; Tolochko, B. P.; Sheromov, M. A. *J. Incl. Phenom*. **2002**, *42*, 213.

(24) Stackelberg, V. M.; Muller, H. R. *Z. Elektrochem*. **1954**, *58*, 25.

(25) Sortland, L. D.; Robinson, D. B. *Can. J. Chem. Eng*. **1964**, *42*, 38.

(26) Manakov, A. Yu.; Larionov, E. G.; Ancharov, A. I.; Mirinskii, D. S.; Kurnosov, A. V.; Dyadin, Yu. A.; Tolochko, B. P.; Sheromov, M. A. *Mendeleev Commun*. **2000**, 235.

(27) Semenova, A. I.; Tsiklis, D. S. *Russ. J. Phys. Chem*. **1975**, *49*, 778.

(28) Ivanov, A. N.; Litvin, D. F.; Savenko, B. N.; Smirnov, L. S.; Voronin, V. I.; Teplykh, A. E. *High Pressure Res*. **1995**, *14*, 209.

(29) Aksenov, V. I. *Prepr. J. Inst. Nucl. Res., Dubna* **1994**, D3−94−364.

(30) Ancharov, A. I.; Manakov, A. Yu.; Mezentsev, N. A.; Tolochko, B. P.; Sheromov, M. A.; Tsukanov, V. M. *Nuclear Instrum. Methods Phys. Res., Sect. A* **2001**, *470*, 80.

(31) Mirinski, D. S.; Manakov, A. Yu.; Larionov, E. G.; Kurnosov, A. V.; Ancharov, A. I.; Dyadin, Yu. A.; Tolochko, B. P.; Sheromov, M. A.; *Nucl. Instrum. Methods Phys. Res., Sect. A* **2001**, *470*, 114.

(32) Goryainov, S. V.; Belitsky, I. A. *Phys. Chem. Miner*. **1995**, 22, 443.

(33) Munro, R. G.; Piermarini, G. J.; Block, S.; Holzapfel, W. B. *J. Appl. Phys*. **1985**, *57*, 165.

(34) Potemkin, V. A.; Bartashevich, E. V.; Belik, A. V. *Russ. J. Phys. Chem*. **1998**, *72*, 4, 561.

(35) Potemkin, V. A.; Sukharev, Yu. I. *Chem. Phys. Lett*. **2003**, *371*, 626.

(36) Taylor, J. C.; Waugh, A. B. *J. Solid State Chem*. **1976**, *18*, 241.

(37) Udachin, K. A.; Ratcliffe, C. I.; Ripmeester, J. A. J. *Phys. Chem. B* **2001**, 105, 4200.

(38) Londono, D.; Finney, J. L.; Kuhs. W. F. *J. Chem. Phys*. **1992**, *97*, 547.

(39) Kuhs, W. F.; Finney, J. L.; Vettier, C.; Bliss, D. V. *J. Chem. Phys*. **1984**, *81*, 3612.

(40) Dyadin, Yu. A.; Bondaryuk, I. V.; Zhurko, F. V. In *Inclusion Compounds*; Atwood, J. L., Davis, J. E. D., MacNicol, D. D., Eds.; Oxford University Press: Oxford, 1991; Vol. 5, p 213

(41) Seryotkin, Yu. V.; Bakakin, V. V.; Fursenko, B. A.; Belitsky, I. A.; Joswig, W.; Radaelli, P. G. *Eur. J. Mineral*. **2005**. *17*, 305.

(42) Manakov, A. Yu.; Goryainov, S. V.; Kurnosov, A. V.; Likhacheva, A. Y.; Dyadin, Yu. A.; Larionov, E. G. *J. Chem. Phys*. **2003**, *107*, 7867.

(43) Stewart, J. W. *J. Chem. Phys*. **1962**, *36*, 400.

(44) Cockroft, J. K.; Fitch, A. N. *Z. Kristallogr*. **1988**, *184*, 123.